# Formation of reactive oxygen species by human and bacterial pyruvate and 2-oxoglutarate dehydrogenase multienzyme complexes reconstituted from recombinant components

Attila Ambrus[a], Natalia S. Nemeria[b], Beata Torocsik[a], Laszlo Tretter[a], Mattias Nilsson[a], Frank Jordan[b], and Vera Adam-Vizi[a,*]

[a]Department of Medical Biochemistry, MTA-SE Laboratory for Neurobiochemistry, Semmelweis University, Budapest, 1094, Hungary

[b]Department of Chemistry, Rutgers, the State University, Newark, NJ 07102, USA

[*]To whom correspondence should be addressed at: Department of Medical Biochemistry, Semmelweis University, 37-47 Tuzolto Street, Budapest, 1094, Hungary. Tel.: +361 266 2773, Fax.: +361 267 0031, E-mail: adam.veronika@med.semmelweis-univ.hu

**Abstract**

Individual recombinant components of pyruvate and 2-oxoglutarate dehydrogenase multienzyme complexes (PDHc, OGDHc) of human and *Escherichia coli* (*E. coli*) origin were expressed and purified from *E. coli* with optimized protocols. The four multienzyme complexes were each reconstituted under optimal conditions at different stoichiometric ratios. Binding stoichiometries for the highest catalytic efficiency were determined from the rate of NADH generation by the complexes at physiological pH. Since some of these complexes were shown to possess 'moonlighting' activities under pathological conditions often accompanied by acidosis, activities were also determined at pH 6.3. As reactive oxygen species (ROS) generation by the E3 component of hOGDHc is a pathologically relevant feature, superoxide generation by the complexes with optimal stoichiometry was measured by the acetylated cytochrome c reduction method in both the forward and the reverse catalytic directions. Various known affectors of physiological activity and ROS production, including $Ca^{2+}$, ADP, lipoylation status or pH, were investigated. The human complexes were also reconstituted with the most prevalent human pathological mutant of the E3 component, G194C and characterized; isolated human E3 with the G194C substitution was previously reported to have an enhanced ROS generating capacity. It is demonstrated that: *i.* PDHc, similarly to OGDHc, is able to generate ROS and this feature is displayed by both the *E. coli* and human complexes, *ii*. Reconstituted hPDHc generates ROS at a significantly higher rate as compared to hOGDHc in both the forward and the reverse reactions when ROS generation is calculated for unit mass of their common E3 component, *iii.* The E1 component or E1-E2 subcomplex generates significant amount of ROS only in hOGDHc; *iv.* Incorporation of the G194C variant of hE3, the result of a disease-causing mutation,

into reconstituted hOGDHc and hPDHc indeed leads to a decreased activity of both complexes and higher ROS generation by only hOGDHc and only in its reverse reaction.

**Keywords**

2-oxoglutarate dehydrogenase complex; alpha-ketoglutarate dehydrogenase complex; pyruvate dehydrogenase complex; reactive oxygen species; E3 deficiency; oxidative stress

## Abbreviations

OGDHc, 2-oxoglutarate (also known as alpha-ketoglutarate) dehydrogenase complex; PDHc, pyruvate dehydrogenase complex; OG, 2-oxoglutarate; cyt *c*, cytochrome *c*; LA, lipoic acid; EDTA, ethylene diamine tetraacetic acid; FAD, flavin adenine dinucleotide; LADH, (dihydro)lipoamide dehydrogenase (E3 component); MW, molecular weight; $NAD^+$/NADH, nicotinamide adenine dinucleotide (oxidized/reduced forms); ROS, the reactive oxygen species superoxide anion and hydrogen peroxide; SOD, superoxide dismutase; Tris, 2-amino-2-hydroxymethyl-propane-1,3-diol; wt, wild-type; ThDP, thiamin diphosphate; CoA, Coenzyme A; ec, *E. coli* origin; h, human origin.

## Introduction

Pyruvate and 2-oxoglutarate (OG, also known as α-ketoglutarate) dehydrogenase complexes (PDHc/OGDHc or KGDHc) are central enzymes in all forms of aerobic metabolism catalyzing the oxidative decarboxylation of pyruvate and OG, respectively, generating NADH. Although the mechanisms of action and metabolic roles of these enzymes have long been established [1-6], they continuously regain interest due to the new pathological aspects and moonlighting activities discovered in the last decade [7-13]. The implications of OGDHc in oxidative stress were recently reviewed [14, 15].

PDHc and OGDHc consist of three major components: E1 (pyruvate/2-oxoglutarate dehydrogenase, EC 1.2.4.1/1.2.4.2), E2 (dihydrolipoyl (or dihydrolipoamide) transacetylase/transsuccinylase (or acetyl/succinyltransferase), EC 2.3.1.12/2.3.1.61), and E3 (dihydrolipoyl (or (dihydro)lipoamide) dehydrogenase, EC 1.8.1.4) [3, 16-22]. The E3 component (lipoamide dehydrogenase, LADH) is common to both complexes in the same cell [23, 24], but LADH is also part of the branched-chain keto-acid dehydrogenase complex and the glycine cleavage system [1]. There are differences among the prokaryotic and eukaryotic enzymes and also between the respective PDH and OGDH complexes in minor but functionally important additional components, the number of lipoyl domains and subunit stoichiometry (see Results and *SI*) [2, 3, 16, 25], showing the versatility of these multienzyme complexes as well as the possibility of fine-tuning their function through structural assembly, in different biochemical environments.

The overall dehydrogenase reactions by PDHc or OGDHc are irreversible, although when NADH is in excess both complexes consume NADH in a reverse reaction catabolized by E3 [26] (see below).

The isolated mammalian (porcine heart) OGDHc and PDHc were shown to generate superoxide anion radical and hydrogen peroxide under pathologically relevant conditions (high NADH/$NAD^+$ ratio, acidosis) [7, 8, 27] and OGDHc was reported to serve as a major source of oxidative stress related to senescence/aging, ischemia-reperfusion or neurodegeneration [7, 8, 14, 15, 27-37]. OGDHc is not only a source but also a sensitive target of reactive oxygen species (ROS) in mitochondria [5, 38-41]; hypoxia- and glutamate-induced cerebral damage was strongly linked to the inactivation of OGDHc [34]. The mammalian PDHc was demonstrated to be a much weaker ROS generator compared to OGDHc [7, 11, 13]; the reason for this still appears obscure [13, 36, 42]. PDHc is also sensitive to ROS, and its functional integrity is implicated to be important for neuronal longevity and survival [43, 44]. ROS generation by prokaryotic OGDHc or PDHc and its potential role have not been investigated before.

Earlier, ROS generation by OGDHc and PDHc was ascribed to the E3 flavoenzyme component (LADH) [7, 8]; ROS generation by LADH has been addressed in several studies using isolated (mammalian) LADH or *in silico* approaches [26, 27, 31, 37, 42, 45-50]. It was found that ROS production by LADH is potentiated by $Zn^{2+}$ [47], acidosis [27], is relevant to ischemia/reperfusion and possibly to Alzheimer's disease (for $Zn^{2+}$). LADH's specific disease-causing mutations [37, 42, 45, 50] are relevant to multiple pathologies related to E3-deficiency (collected most recently in [51]). Although the primary site for ROS generation in PDHc and OGDHc had been ascribed to the E3

component [7, 8], there are recent results suggesting the potential involvement of the E1 component, or perhaps even of the E2 component: the isolated E1o (o for OGDHc) component of *E. coli* (ecE1o) as well as the E1p (p for PDHc) component of *Bacillus stearothermophilus* have been shown to generate $H_2O_2$ through radical formation *via* the thiamin diphosphate (ThDP) cofactor [52] and our groups have recently reported superoxide and $H_2O_2$ generation by the human E1o component [12]. It should be noted that other enzymes dependent on ThDP have also been found to generate stable radicals by ThDP, such as pyruvate ferredoxin oxidoreductase and pyruvate oxidase [53]. The E3 component is bound to PDHc ~30 times stronger than to OGDHc [54-56], and there are indications that LADH may exist, and potentially generate ROS, as an independent enzyme [25, 27, 54, 57, 58]. Involvement of the E1-E2 sub-complexes of mammalian 2-oxoacid dehydrogenase complexes in ROS generation was speculated based upon indirect findings [27, 59], but could not be examined earlier in the absence of pure isolated components of the complexes.

In this study we expressed in *E. coli* and purified all components of both human and *E. coli* OGDHc and PDHc. We determined the catalytic and the superoxide-generating activities of the reconstituted complexes under various conditions to address: *i.* The optimal stoichiometry of components leading to the highest catalytic activity, *ii*. The effect of pH and several other known regulators (lipoylation status, $Ca^{2+}$, ADP) on the catalytic activities, *iii.* The effect of different levels of reconstitution (E1, E1-E2, E1-E2-E3) and known regulators (see above) on superoxide generation in the forward and the reverse modes for each complex, *iv.* A quantitative comparison of superoxide generation by OGDHc *versus* PDHc and their respective prokaryotic *versus* eukaryotic

complexes, and *v.* The effect of the most prevalent human pathological mutation of the E3 component, G194C on the activity and superoxide generation by PDHc or KGDHc.

## Materials and Methods

*Protein Expression and Purification*

The methods for overexpression and purification of *E. coli* E1p, 1-lip E2p and E3 components were described earlier [60-62]. Overexpression and purification of the *E. coli* E1o, E2o and E3 components was also as reported earlier [63]. The human PDHc components were expressed and purified as reported in the literature (E1p [64], E2p.E3BP [65-67], E3 [68], and Gly194Cys E3 [37]). The human E1o, E2o (and E3) components were expressed and purified as reported recently [12]. Lipoyl ligase was expressed and purified as before [69]

*Reconstitution of the Multienzyme Complexes*

In this paper, for the purpose of enzymatic activity measurement, the mass ratio (μg: μg: μg) of the individual components assembled into complexes was applied rather than the molar ratio of their subunits (μM: μM: μM), both of which have been reported in the literature. Generally, the mass ratio (μg: μg: μg) of 1:1:1 was tested first and then conditions of component assembly were optimized for each complex individually, taking into account the subunit stoichiometry reported in the literature (see Supporting Information for reconstitution of each individual complex and the corresponding Figure Legends).

*Measurement of Enzyme Activity*

*NADH production by pyruvate and 2-oxoglutarate dehydrogenase complexes*. The experiments for measurement of the overall complex activity were designed taking into consideration the pH optimum of the reaction for each individual complex, the values of $K_m$ for pyruvate and 2-oxoglutarate and the values of $K_m$ for ThDP also reported in the literature [70-78]. The initial rate of NADH production by the complexes was detected at 340 nm in EIA/RIA 96-well, flat-bottom, polystyrene plates (Corning, Lowell, MA, USA) using a Spectramax M2 (Molecular Devices, Sunnyvale, CA, USA) or a Victor 3 (Perkin Elmer, Waltham, MA, USA) multi-label counter spectrophotometer/fluorimeter at 37 $^{o}$C. Assay conditions were the following in a 300 μL final reaction volume: 50 mM $K_2HPO_4$ (pH 7.3 or 6.3), 0.2 mM ThDP, 2.5 mM $NAD^+$, 1 mM $Mg^{2+}$, 0.1 mM CoA, and 2 mM pyruvate or 2 mM 2–oxoglutarate according to the reaction: pyruvate/2-oxoglutarate + $NAD^+$ + CoA → acetyl/succinylCoA + NADH. E3 (0.1 μg) was used in each well for consistent results unless otherwise mentioned in specific experiments. The reaction was initiated after 15 min of pre-incubation of the assay mixture at 37 $^{o}$C (to obtain a stable base line) by addition of the reconstituted complexes (total of 2 μL, 0.67% of the total volume) and subsequent addition of CoA (5 μL, 1.67% of the total volume). Five parallel experiments were carried out for most measurements. The molar extinction coefficient (ε) for NADH was estimated under our experimental conditions and an $\varepsilon_{340}$ = 4,646 $M^{-1}cm^{-1}$ (pH 7.3) and $\varepsilon_{340}$ = 4,856 $M^{-1}cm^{-1}$ (pH 6.3) were calculated (an $\varepsilon_{340}$ = 6,220 $M^{-1}cm^{-1}$ was reported in the literature [79]). To obtain a linear initial velocity curve, 1 mM DTT (2 μl) was added to the assay with human PDHc, however DTT was omitted from the superoxide detection assay because cytochrome *c* (cyt *c*) proved to be sensitive to DTT.

*Superoxide Detection in the Physiological Direction.* Superoxide generation by the reconstituted complexes was measured *via* reduction of partially acetylated cyt *c*, as described earlier [37, 80-83], with minor modifications. In the physiological direction the assay mixture has the same composition as for the NADH assay presented above, with the exception of the 200 μL of assay volume containing 50 mM $K_2HPO_4$ (pH 6.3), 50 μM cyt *c* [37, 80], calculated amounts from the reconstituted complexes (containing generally 2 μg of E3 component) and omitting $NAD^+$, according to the reaction scheme: pyruvate/2-oxoglutarate + (ec/h)PDHc/OGDHc + $Mg^{2+}$ + ThDP + CoA + $O_2$ → superoxide (detected by cyt c). Superoxide detection was initiated by the addition of 2 mM pyruvate or 2 mM 2-oxoglutarate (10 μL, 5% of the volume) due to the higher volume (generally 40 μL) of the protein complexes needed because of the low sensitivity of the cyt *c* assay. The initial reaction velocity was measured and converted to the amount of the superoxide generated *per* unit time *per* mg protein, taking into account a 1:1 stoichiometry of the reaction between cyt *c* and superoxide [80].

*Superoxide detection in the non-physiological reverse direction*. In the reverse direction, solution conditions were the following in 200 μl final reaction volume: 50 mM $KH_2PO_4$ (pH 6.3), 50 μM acetylated cyt *c*, 165 μM NADH (3.3 μL, 1.7% of the volume), 0.2 mM ThDP, 1 mM $Mg^{2+}$ and calculated amounts from the reconstituted complexes (containing generally 2 μg of E3 component), unless otherwise stated, according to the reaction scheme: NADH + (ec/h)PDHc/OGDHc + $Mg^{2+}$ + ThDP + $O_2$ → superoxide (detected by cyt c) . Pyruvate, 2-oxoglutarate and CoA were omitted from the reaction assay [8]. A

lower than physiological pH was applied in all experiments for superoxide detection due to the greatly enhanced ROS production by the complexes, especially in the reverse reaction, at pH<7.0; this condition also mimics acidosis that generally accompanies ROS production by the complexes under pathological conditions [27, 37, 51, 84]. Measurements were carried out at 37 $^{o}$C at the absorbance maximum of 550 nm of the reduced form of acetylated cyt *c*, similarly to that used in the physiological direction. The reaction was initiated by the addition of NADH after 15 min incubation at 37 $^{o}$C. The extinction coefficient of the reduced cytochrome *c* was determined by fully reducing oxidized cyt *c* under the assay conditions by sodium dithionite, providing an $\varepsilon_{550}$=10,172 $M^{-1}cm^{-1}$. Superoxide dismutase from bovine erythrocytes (SOD) was used to verify that cyt *c* reduction was indeed caused by superoxide generated by the enzymes; 100 U SOD were added to 200 μL of reaction assay where applied. Five parallel experiments were carried out for most measurements.

*Statistics.* Statistical differences were evaluated in Excel with two-tailed Student's t-tests assuming unequal variances and were accepted to be significant when $P < 0.05$.

## Results

*Superoxide production by E. coli pyruvate and 2-oxoglutarate dehydrogenase complexes.*

*Superoxide production by E. coli PDHc and its components.* As displayed in Fig. 1, the assembled ecPDHc produces superoxide from pyruvate (forward physiological direction) with a rate of 41.4 nmol·min$^{-1}$·mg E3$^{-1}$. In the presence of pyruvate, $NAD^+$, CoA and all three components assembled into PDHc, the major products would be NADH and acetyl-CoA (overall activity of NADH production of 20.7 units/mg E3 at 1:1:1 component mass ratio and of 34.7 units/mg E3 at 3.98:2.72:1 mass ratio was measured, Fig. S1; the latter mass ratio was calculated using a molar ratio of subunits and mass of subunits from the literature - see *SI*), and superoxide production could be considered as a side reaction (0.12% at 3.98:2.72:1 mass ratio of E1p:E2p:E3 components). As is also evident from Fig. 1, the E1p on its own and the corresponding E1p-E2p sub-complex do not produce any significant amount of superoxide, suggesting that E3 is responsible for superoxide production in both the forward and the reverse (non-physiological) reactions, as expected from earlier reports [7, 8, 27]. It is well accepted that E3 catalyzes the transfer of reducing equivalents from dihydrolipoamide (covalently amidated onto E2) to $NAD^+$ in the physiological direction *via* FAD and a disulfide redox center on E3, resulting in lipoamide-E2 and NADH. In the reverse direction, NADH reduces FAD and the disulfide exchange site on E3 which with oxygen first leads to superoxide and then to $H_2O_2$ by dismutation of the former [48, 85]. Generation of radical species by flavoenzymes, including dihydrolipoamide dehydrogenase, is well-established [7, 8, 27, 37, 47-49, 86]. As expected, the E3 component by itself also produced superoxide [27, 37] in the reverse direction, as indeed could the assembled PDHc (Fig, 1, bars 2 and 4). This rules out the

need for E2p in ROS production, rather it implicates the two proximal cysteines in E3, known to undergo reversible oxidation-reduction and assisting in the formation of a redox couple with FAD, and FAD itself (see above).

The activity of superoxide production by ecE3 (75.4 nmol·min$^{-1}$·mg E3$^{-1}$) and by ecPDHc (62.0 nmol·min$^{-1}$·mg E3$^{-1}$) in the reverse reaction were of comparable magnitudes, clearly indicating that E3 is the major source of superoxide production on the entire *E. coli* PDHc. It is also notable that the reactivity of superoxide generation by ecPDHc in the physiological direction of 41.4 nmol· min$^{-1}$· mg E3$^{-1}$ is much less than in the reverse reaction (62.0 nmol· min$^{-1}$· mg E3$^{-1}$), and the difference could be due to the different kinetics (and mechanisms) of superoxide generation by ecE3 in the two directions.

The novelty of this section is the first demonstration that *E. coli* PDHc could generate superoxide in both the physiological and the reverse non-physiological directions. In the physiological direction with pyruvate as substrate, superoxide generation represents 0.12 % of the NADH production. The E3 component is the major source of superoxide generation by *E. coli* PDHc: neither the E1p component nor the E1p-E2p sub-complex alone generated detectable amounts of superoxide.

*Superoxide generation by E. coli 2-oxoglutarate dehydrogenase complex*. Similarly to *E. coli* PDHc, the *E. coli* OGDHc generates superoxide in the physiological direction with a rate of 19.0 nmol·min$^{-1}$·mg E3$^{-1}$ when OGDHc was assembled at a mass ratio of either 2.07:0.86:1 or 2.07:1.72:1 (Fig. 2, also see Fig. S2 and *SI*). On comparison with ecPDHc (41.4 nmol· min$^{-1}$· mg E3$^{-1}$), ecOGDHc produces superoxide at one half the rate (19.0 nmol·min$^{-1}$·mg E3$^{-1}$) representing 0.58% of the rate of NADH production (3.26

μmol·min$^{-1}$·mg E3$^{-1}$). In the reverse direction, the activity of 44.7 nmol·min$^{-1}$·mg E3$^{-1}$ (ecOGDHc at the 2.07:0.86:1 mass ratio) was comparable to the 62.0 nmol·min$^{-1}$·mg E3$^{-1}$ by ecPDHc, and to the one by ecE3 (75.4 nmol·min$^{-1}$·mg E3$^{-1}$), again confirming that the E3 component is responsible for superoxide production, a component that is common to both complexes. *In vitro* lipoylation gave an apparent reduction in superoxide formation by ecOGDHc in the forward direction, while increasing it in the reverse direction, an observation that needs further scrutiny. The rate of superoxide generation in the reverse reaction was significantly higher when measured with the putative complex of 2.07:0.86:1 mass ratio (12:12:12 chain stoichiometry; bar 3 *versus* bar 7 in Fig. 2) which shows that the presence of excess E3 could indeed result in an increased superoxide generation with NADH (see Fig. 1); uncomplexed E3 can produce superoxide generally stronger than when in the complex [27].

Concluding about superoxide production by ecOGDHc: Superoxide is generated in the physiological direction. It was demonstrated by others that isolated ecE1o could generate hydrogen peroxide [52]. Also, formation of ThDP-enamine radical intermediate was demonstrated by EPR spectroscopy. It was suggested that one electron reduction of oxygen by the ThDP-enamine intermediate could lead to ThDP-enamine radical + superoxide [12, 52], indicating that the ThDP-enamine intermediates could undergo radical chemistry that is different from that carried out by the E3 component. However, under our experimental conditions no superoxide generation was detected for ecE1o on its own or for E1o-E2o sub-complex. Our results do not rule out that ecE1p or ecE1o could generate superoxide or $H_2O_2$, they probably reflect the fact that the colorimetric cyt

c assay possesses far less sensitivity compared to the Amplex assay (which is based on fluorimetric detection of hydrogen peroxide) used in Frank et al, 2008 [87].

*Superoxide generation by human pyruvate and 2-oxoglutarate dehydrogenase complexes.*

*Superoxide generation by hPDHc*. It was demonstrated that hPDHc generates superoxide in the physiological direction with activity of 56.7 nmol· $min^{-1}$ ·mg $E3^{-1}$ that represents about 0.15% of the overall hPDHc activity (37 μmol ·$min^{-1}$· mg $E3^{-1}$) at a mass ratio of hE1p:hE2p.E3BP:hE3 = 7.52:5.77:1 (Fig. 3 and *SI*). In the reverse direction with the same assembly of components, the superoxide activity of hPDHc was 108.3 nmol· $min^{-1}$· mg $E3^{-1}$ and was similar to that of the isolated hE3 (96.1 nmol· $min^{-1}$ ·mg $E3^{-1}$) in the reverse direction. The result is in agreement with data reported from the Adam-Vizi laboratory earlier [37]. The data above clearly indicate that hE3 assembled into hPDHc could produce superoxide with efficiency similar to that of the isolated hE3. Since no superoxide generation was detected with either hE1p or hE1p-hE2.E3BP sub-complex in the absence of hE3 (data not shown), the superoxide generation by hPDHc in the physiological direction could be attributed to hE3.

Superoxide generation by isolated G194C hE3 was about two-fold higher than that for wt hE3 (191.6 nmol· $min^{-1}$ ·mg $E3^{-1}$, not shown in figure) and was in accordance with data reported from the Adam-Vizi laboratory earlier [37]. Next, the G194C substituted hE3 was reconstituted with hE1p and hE2p.E3BP sub-complex. In the forward physiological direction this hPDHc displayed lower superoxide activity (Fig. 3) (42.5 nmol· $min^{-1}$ ·mg $E3^{-1}$) as compared with superoxide activity of 56.7 nmol· $min^{-1}$ ·mg $E3^{-1}$ detected for hPDHc reconstituted with wt E3 (compare bars 2 and 4 in Fig. 3).

However, there was no statistically significant difference between the rates of superoxide production in the reverse direction (compare bars 3 and 5 in Fig. 3).

The superoxide generating activity of the complex reconstituted with the G194C variant of hE3 measured in the reverse non-physiological direction was also similar in magnitude to that of the uncomplexed hE3 (bars 1 and 5 in Fig. 3).

*Superoxide generation by hOGDHc*. On reconstitution of hOGDHc from hE1o, hE2o, and hE3 components with a mass ratio of 4.30:1.68:1, an overall NADH producing activity of 0.625 μmol·min$^{-1}$·mg E3$^{-1}$ was detected at maximum efficiency (Fig. S4). Similarly to the *E. coli* complexes and to hPDHc, the hOGDHc was effective in generating superoxide with an activity of 12.1 nmol ·min$^{-1}$ ·mg E3$^{-1}$ in the forward physiological direction (1.9% of the overall OGDHc reaction of NADH production) and 40.5 nmol· min$^{-1}$· mg E3$^{-1}$ in the reverse reaction (Fig. 4), again significantly higher than in the forward physiological direction (compare bars 2 and 1 in Fig. 4).

What distinguishes hOGDHc from the other complexes discussed, is that the hE1o and hE1o-hE2o sub-complex, even in the absence of hE3, were still able to generate superoxide in the forward physiological direction with the following rates: 2.06 nmol· min$^{-1}$ ·mg E1o$^{-1}$ for hE1o on its own and 1.76 nmol· min$^{-1}$ ·mg E1o$^{-1}$ for the hE1o-hE2o sub-complex (bars 5 and 6 in Fig.4). The results suggest that hE2o may not contribute to superoxide generation. It had been suggested for porcine heart OGDHc [27, 88] that superoxide could also be generated by E2o *via* a thiyl radical in the absence of E3, but our results provide still no clear evidence for this [59].

As was reported by our groups, the ThDP-enamine radical could be detected by EPR using hE1o by itself, or hE1o assembled into hOGDHc. The concentration of ThDP-

enamine radical was 0.9 μM for hE1o (0.2% occupancy of active centers) and 1.3 μM for hE1o assembled into hOGDHc (0.59% occupancy of active centers) [12]. The data here reported clearly demonstrate first the important difference between hOGDHc and hPDHc, and second between human and prokaryotic OGDHc complexes. The ThDP-enamine radical is the likely source of superoxide on free hE1o, while ROS generation by the intact OGDHc was ascribed to the E3 component [7, 8]. Reconstitution of the human OGDHc with Gly194Cys substituted E3 (result of a pathogenic mutation) resulted in a statistically significant (21.5%) decrease in superoxide generation in the forward physiological direction (compare bar 3 *versus* bar 1 in Fig. 4), whereas in the reverse E3 reaction a (statistically significant) 11.3% increase was observed upon this disease-causing amino acid substitution (compare bars 4 and 2 in Fig. 4).

## Discussion

ROS generation by hOGDHc is heavily implicated in the progression of neurodegenerative diseases, such as Alzheimer's and Parkinson's disease, infantile lactic acidosis, and Friedreich's ataxia, among others [5, 28, 32, 35, 36, 84, 89-92].

This is the first study to demonstrate that ecPDHc and ecOGDHc could produce superoxide. Given the similar observations made earlier with mammalian enzymes [7, 8, 27], it can now be stated that 2-oxo acid dehydrogenase complexes, in general, possess the ability of ROS generation, in particular, under pathologically relevant conditions (acidosis, high NADH/$NAD^+$ ratio and/or when the physiological $e^-$-acceptor is absent or present only at small concentrations). Given that E3 is likely the primary site for ROS production by the intact complexes [7, 8], and that ecE3 and hE3 show a high degree of sequence similarity (44% identity), this generalized concept always seemed reasonable, but had not been experimentally investigated or proven before. The results for the prokaryotic enzymes show that ecPDHc is just as much, if not more efficient as a superoxide producer as ecOGDHc *in vitro*. Obviously, substrate and cofactor availability under physiological or pathological conditions may modulate these catalytic efficiencies and their ratios *in vivo* [13]. We also found that both prokaryotic complexes generate more superoxide in the reverse than in the forward reactions, similarly to the eukaryotic enzymes, implying that the mechanisms are likely similar. Neither prokaryotic sub-complexes (ecE1p/o, ecE1p/o-ecE2p/o) exhibited detectable superoxide generating activity under our assay conditions, which, in the case of ecOGDHc is a marked difference relative to the eukaryotic enzyme. The fact that the prokaryotic 2-oxo acid dehydrogenase complexes are also able to generate ROS implies that this feature

remained an inherent property of these enzymes throughout evolution. This highly conserved mechanism may have similar implications in prokaryotes to the ones in eukaryotes, such as self-regulation (e.g., for metabolic enzymes such as OGDHc [88]), signal transduction (e.g., regulation by transcription factors [36, 89, 93]), or defense (e.g., by cytotoxic lymphocytes in mammals [94]). Obviously, over-production of ROS may lead to cellular damage in any organism or tissue [28-30, 36, 95].

In the human brain, the activity of OGDHc is a rate-limiting step in the Krebs cycle [1, 2, 4, 5, 76, 96] and the activity of hPDHc was found to be five-fold higher than that of hOGDHc [97]. This ratio was ~3 (mitochondrion) or ~7 (intact cell) in fibroblasts and ~1.5 (mitochondrion) or ~15 (intact cell) in leukocytes [98]. In alamethicin permeabilized rat brain mitochondria the activities of the two enzymes were nearly identical [7]. Measurements with the reconstituted human enzymes in our study demonstrate that hPDHc (37 unit/mg E3) was ~59 times more active than hOGDHc (0.625 unit/mg E3). Superoxide activity in the forward reaction was ~ 5-fold higher for hPDHc than hOGDHc, whereas in the reverse reaction hPDHc generated superoxide at a ~2.5-fold higher rate as compared to hOGDHc when this activity was calculated for the unit amount of their common E3 subunit. The higher physiological activity of hPDHc (relative to that of hOGDHc) is in accord with literature data (see above). The higher (both forward and reverse reactions) superoxide generating capacities of hPDHc relative to those of hOGDHc also applies to the prokaryotic complexes in this study, but not to the isolated porcine equivalents studied earlier [7, 8], which Sigma preparations however proved to be of questionable purities in our hands. In a broader sense, we propose that potentially all 2-oxo acid dehydrogenase complexes should be considered as potent ROS

generating enzymes, although *in vivo* conditions and their transcriptionally/translationally determined total amounts may considerably modulate their efficiency to contribute to the gross ROS production of mitochondria or cells [13].

Complex I isolated from bovine heart mitochondria produced 42.1 $nmol.min^{-1}.mg^{-1}$ superoxide in a NADH supported ROS generation assay [99]. Succinate dehydrogenase (Complex II) was also tested *in vitro* in bovine heart submitochondrial particles where ~10 $nmol.min^{-1}.mg^{-1}$ activity was found in an $H_2O_2$ detection assay [100, 101]. Another isolated ROS producer, the membrane-bound dihydroorotate dehydrogenase purified from rat liver mitochondria was also assessed, but the ROS producing activity was not clearly quantified [102]. The above reported values for isolated ROS producing enzymes show a similar order of magnitude when compared to the ROS production rates exhibited by hPDHc or hOGDHc in this study. Rigorous quantitative comparison of literature values of other ROS producing sites to the values reported here for hPDHc or hOGDHc is difficult to obtain due to considerable differences in the applied assay conditions; comparison or projection of *in situ/in vivo* results to *in vitro* data (measured with purified proteins) and *vice versa* is also heavily error prone [103]. A recent more reliable comparison for *in vivo* relevance of *in situ* ROS production rates displayed by Complex I, PDHc and OGDHc in isolated rat skeletal muscle mitochondria showed that superoxide/$H_2O_2$ was produced by the OGDHc at a two-fold higher rate than PDHc, and at eight-fold rate compared to site $I_F$ of Complex I [13]. The *in vivo* or *in situ* capacities, under selected experimental conditions, of the various ROS producing sites revealed so far have been thoroughly documented, partly by our laboratory [91, 104-110], and recently reviewed in [103].

The fact that the uncomplexed hE1o, as well as the hE1o-hE2o sub-complex could generate superoxide in the forward reaction comparable to that generated by hOGDHc, is of particular interest. This is a marked difference from what we found with the other three complexes, which exhibited no measurable superoxide generation when lacking the respective E2/E3 or just the E3 components. Plausible mechanistic explanation for the above observation concerning hE1o were suggested in our recent study [12], suggesting differences in the stabilities of respective ThDP-bound post-decarboxylation catalytic intermediates on hOGDHc and hPDHc (Scheme 1). ROS (superoxide and $H_2O_2$) generation by hE1o, first reported recently [12], might have pathological relevance under conditions where the stoichiometric assembly of the hOGDHc is compromised and hE1o is present in excess inside mitochondria [21, 111-115]. Earlier, it was concluded that for ROS generation by the mammalian OGDHc, the E3 component was solely responsible [7, 8]. As the E1o-E2o subcomplex is far more stable than the (E1o-E2o)-E3 complex for OGDHc [54-56], the above condition may result from genetic deficiencies of hE2o (for further discussion, see [12]). ROS generation by the hE1o-hE2o subcomplex may have potential relevance (under certain pathological conditions), as E3 binds ~30 times less tightly to OGDHc than to PDHc [54-56], and this may be more pronounced in acidosis [27]. We propose that in acidosis, uncomplexed E3 in the reverse reaction, as well as the E1o-E2o subcomplex in the forward reaction might generate ROS, provided that sufficiently high concentrations of NADH or OG, respectively are available. This new mechanistic view may be worth considering in targeting ROS generation by OGDHc, but additional investigations are needed to further characterize ROS generation by this subcomplex. Scheme 1 provides a

summary of the known sites of superoxide generation on the hOGDHc subcomplexes and the fully assembled 2-oxoacid dehydrogenase complexes in general according to the current literature [12, 47, 48, 85].

Since the G194C pathogenic amino acid substitution of hE3 [116-118] is usually accompanied by lactic acidosis, it was important to address the activity of hPDHc with this substitution at pH 6.3. This pathogenic substitution led to an 87% decrease in the overall assay (see *SI* and Fig. S3, bars 4 and 7), in good agreement with the 80-90% loss of hPDHc activity found in patients with either heterozygote or homozygote mutations [84, 116, 118]. The activity of hOGDHc similarly diminishes under conditions *in* vitro when the complex is reconstituted with the G194C hE3 (*SI* Fig. S4). It is also important to emphasize that the isolated hE3 G194C did not display significant loss of activity either in the forward or the reverse reaction, but showed a significantly enhanced superoxide generation in the reverse reaction [37]. An elucidation of the mechanism by which hE3 with the G194C substitution decreases the overall PDHc and OGDHc activities will be the subject of further investigations. There are a few pathogenic mutations of hE3 that impede the recruitment of hE3 to hE3BP (in hPDHc) [119]; this may also occur with hE3 G194C thus offering a plausible explanation for the above findings. It is noteworthy that the presence of hE3 G194C lowered superoxide generation in the forward direction for both complexes to a similar extent (~20%), pointing to a potentially similar mechanism. In the reverse reaction it did not alter superoxide generation by hPDHc, whereas it significantly (~11%) increased superoxide production by hOGDHc; the augmented ROS production by hOGDHc containing hE3 G194C may also contribute to the cellular/tissue damage associated with this mutation. These results

complement a previous report on isolated hE3 G194C [37], which showed significantly enhanced (>70%) ROS generation due to this substitution.

It is clear from the present results that the G194C hE3 substitution substantially reduces, by a hitherto unelucidated mechanism, primarily the activity of PDHc, but also that of OGDHc, while its own catalytic activity is essentially unchanged [37], and results in an excess ROS generation in the reverse reaction by hOGDHc. However, hE3 G194C generates ROS at an even higher rate when it is present uncomplexed [27, 57, 58].

The present findings add to our understanding of the molecular pathology of 2-oxo acid dehydrogenase complexes in general, and to that of hPDHc and hOGDHc in particular, with both complexes being potentially involved in the mechanisms of neurodegenerative diseases.

**Acknowledgments**

We are grateful to Drs. Hetalben Patel, Sowmini Kumaran, Junjie Wang, all from Rutgers, and Da Jeong Shim and Edgardo T. Farinas (New Jersey Institute of Technology) for providing purified proteins to this project, and Mulchand S. Patel and his group for providing cells harboring plasmids of the hPDHc components. Financial support is gratefully acknowledged from the Hungarian Academy of Sciences (MTA grant 02001 to A-V.V.), the Hungarian Scientific Research Fund (OTKA, grant 112230 to A-V. V.), the Hungarian Brain Research Program (grant KTIA_13_NAP-A-III/6. to A-V.V.), the Bolyai and the Fulbright Fellowships (to A.A.), and the NIH (NIH-GM-050380 to F.J.).

**Conflict of Interest statement.** The authors declare no conflict of interest.

**Legends to figures**

**Figure 1. ROS generation by reconstituted ecPDHc under different conditions.** ROS production is expressed as nmol superoxide generated /min/mg of E3 (or E1 for the last two columns). Linear fitting to initial velocity data points generated always an $R^2$>0.96. The primary data were corrected with the average slopes of the blanks. Error bars represent S.E.M. values for three parallel measurements. Statistically significant differences relative to bar 2 are labeled by asterisks (*) ($p<0.05$). Specific conditions are indicated under the charts; Forward direction **F**: superoxide generation by reconstituted complexes in the physiological direction by substrates pyruvate or 2-oxoglutarate in the reaction mixture used for overall activity measurement (see Materials and Methods), but omitting $NAD^+$: pyruvate/2-oxoglutarate + (ec/h)PDHc/OGDHc + $Mg^{2+}$ + ThDP + CoA + $O_2$ → superoxide (detected by cyt c), Reverse direction **R**: superoxide generation by reconstituted complexes in the non-physiological direction using NADH as a substrate, but in the absence of pyruvate or 2-oxoglutarate and CoA: NADH + (ec/h)PDHc/OGDHc + $Mg^{2+}$ + ThDP + $O_2$ → superoxide (detected by cyt c). Other conditions were as detailed in Materials and Methods. pH for superoxide production was 6.3 in all the cases except for measurements with ecPDHc (pH=6.555). For ecPDHc the 3.98:2.72:1 mass ratio was applied for ROS measurement. For ecE1p-ecE2p and ecE1p the same amount of ecE1p and ecE2p were present as for the experiments with ecPDHc.

**Figure 2. ROS generation by reconstituted ecOGDHc under different conditions.** Superoxide production is expressed as for Fig.1. Linear fitting to initial velocity data points generated always an $R^2$>0.92. The primary data were corrected with the average

slopes of the blanks. Error bars represent S.E.M. values for five parallel measurements. Statistically significant differences relative to bar 1 are labeled by single asterisks (*) ($p<0.05$); multiple asterisks label conditions in pairs of particular interest with significant differences to one another (bar 3 to bar 4, bar 5 to bar 6, and bar 7 to bar 8 show significant differences). Conditions are described under the charts. For definitions of **F** and **R** see figure legend 1. The signs - or + lipoylation mean partially or fully lipoylated lipoyl domains of the E2 components. Other conditions were the same as detailed in Materials and Methods. pH was 6.741 in all experiments except for those labeled with $^{\#}$ where the pH was 6.598.

**Figure 3. Superoxide generation by reconstituted hPDHc under different conditions.** Superoxide production is expressed as for Fig.1. Linear fitting to initial velocity data points generated always an $R^2>0.949$. The primary data were corrected with the average slopes of the blanks. Error bars represent S.E.M. values for five parallel measurements. A significant difference exists between bars 2 and 4 (**) ($p<0.05$). Conditions are described under the charts; other conditions were as detailed in Materials and Methods. For definitions of **F** and **R** see figure legend 1. The pH was 6.598 in all experiments except for that labeled with $^{\#}$ where the pH was 6.576 and for uncomplexed hE3 where the pH was 6.300. hPDHc with the 7.52:5.77:1 mass ratio was measured in these experiments. hE3-G194C presented with a 99.4% higher rate of ROS generation relative to hE3 (bar 1) (data not shown).

**Figure 4. ROS generation by reconstituted hOGDHc under different conditions.** Superoxide production is expressed as for Fig.1. Activities are calculated for the mg amounts of the hE3 component except for bars 5 and 6 (labeled with $^{\#}$), where the calculation was made for the amount of hE1o. Linear fitting to initial velocity data points generated always an $R^2$>0.982. The primary data were corrected with the average slopes of the blanks. Error bars represent S.E.M. values for five parallel measurements. Statistically significant differences relative to bar 1 are labeled by single asterisks (*); a significant difference exists also between bars 2 and 4 (**) ($p<0.05$). Conditions are designated under the charts; other conditions were the same as detailed in Materials and Methods. For definitions of **F** and **R** see figure legend 1. In these experiments hOGDHc was reconstituted with the 4.3:1.68:1 mass ratio and the pH was 6.598. For hE1o-hE2o and hE1o the same amount of hE1o and hE2o were present as for the experiments with hOGDHc.

**Figure S1. Overall PDHc activity of reconstituted ecPDHc under different conditions.** Overall activity (NADH production) was measured for the complexes reconstituted from their individually expressed E1, E2, E3 components with the indicated mass ratios. Mass ratios (E1:E2:E3) were: **a.** 1:1:1; **b**. 3.98:2.72:1.0 according to the reaction: pyruvate + $NAD^+$ + CoA → acetylCoA + NADH. The signs - or + lipoylation means partially or fully lipoylated lipoyl domains of the E2 components. Reaction was measured at **c**, pH 7.3 or **d**, pH 6.3. Overall PDHc activity is expressed as μmol NADH/min/mg of the E3 component. Linear fitting to initial velocity data points generated always an $R^2$>0.97. The primary data were corrected with the average slopes of the blanks. Error bars represent S.E.M. values for

five parallel measurements. Statistically significant differences relative to bar 1 are labeled by asterisks (*) ($p<0.05$). See conditions detailed in Materials and Methods.

**Figure S2. Overall OGDHc activity of reconstituted ecOGDHc under different conditions.** Overall activity (NADH production) was measured for the complexes reconstituted from their individually expressed E1, E2, E3 components with the indicated mass ratios. Mass ratios (E1:E2:E3) were: **a.** 1:1:1; **b**. 2.07:0.86:1.0; **c.** 2.07:1.72:1.0 according to the reaction: 2-oxoglutarate + $NAD^+$ + CoA → succinylCoA + NADH. Overall OGDHc activity is expressed as for Fig.S1. Linear fitting to initial velocity data points generated always an $R^2>0.96$. The primary data were corrected with the average slopes of the blanks. Error bars represent S.E.M. values for five parallel measurements. Definitions are described under legend to Figure S1; other conditions were the same as detailed in Materials and Methods.

**Figure S3. Overall PDHc activity of reconstituted hPDHc under different conditions.** Overall PDHc activity is expressed as for Fig.S1. Linear fitting to initial velocity data points generated always an $R^2>0.992$. The primary data were corrected with the average slopes of the blanks. Error bars represent S.E.M. values for five parallel measurements. Statistically significant differences relative to bar 1 are labeled by single asterisks (*) ($p<0.05$). Further comparisons of particular interest were also performed: significant differences also exist for bar 3 to bar 4 (**), for bar 4 to bars 5, 6 & 7 (***; but not to bar 8), and for bar 5 to bar 7 (****). Definitions are described in legend to Figure S1; other conditions were the same as detailed in Materials and Methods.

**Figure S4. Overall OGDHc activity of reconstituted hOGDHc under different conditions.** Overall OGDHc activity is expressed as for Fig.S1. Linear fitting to initial velocity data points generated always an $R^2$>0.991. The primary data were corrected with the average slopes of the blanks. Error bars represent S.E.M. values for five parallel measurements. Statistically significant differences relative to bar 1 (calculated only for bars 2 or 3) are labeled by single asterisks (*); further comparisons of particular interest were also performed: significant differences also exist for bar 3 to bars 4, 5, 8 & 9 (**; but not to bars 6, 7, 10 & 11) and for bar 5 to bar 9 (***) ($p<0.05$). Definitions are described under legend to Figure S2; other conditions were the same as detailed in Materials and Methods. $Ca^{2+}$ was applied in 20 μM or 60 μM concentrations whereas ADP in 0.4 mM or 1.2 mM concentrations, as indicated.

**Scheme 1. Known sites of superoxide generation on the hOGDHc subcomplexes and the fully assembled 2-oxoacid dehydrogenase complexes in general.**

## References


[1] Massey, V. The composition of the ketoglutarate dehydrogenase complex. *Biochim. Biophys. Acta* **38:**447-460; 1960.

[2] Reed, L. J. Multienzyme complexes. *Acc. Chem. Res.* **7:**40-46; 1974.

[3] Perham, R. N. Domains, motifs, and linkers in 2-oxo acid dehydrogenase multienzyme complexes - a paradigm in the design of a multifunctional protein. *Biochemistry* **30:**8501-8512; 1991.

[4] Sheu, K. F. R.; Blass, J. P. The alpha-ketoglutarate dehydrogenase complex. *Oxidative/Energy Metabolism in Neurodegenerative Disorders*. New York: New York Acad Sciences; 1999: 61-78.

[5] Gibson, G. E.; Park, L. C. H.; Sheu, K.-F. R.; Blass, J. P.; Calingasan, N. Y. The [alpha]-ketoglutarate dehydrogenase complex in neurodegeneration. *Neurochem. Int.* **36:**97-112; 2000.

[6] Patel, M. S.; Nemeria, N. S.; Furey, W.; Jordan, F. The Pyruvate Dehydrogenase Complexes: Structure-based Function and Regulation. *J. Biol. Chem.* **289:**16615-16623; 2014.

[7] Starkov, A. A.; Fiskum, G.; Chinopoulos, C.; Lorenzo, B. J.; Browne, S. E.; Patel, M. S.; Beal, M. F. Mitochondrial alpha-ketoglutarate dehydrogenase complex generates reactive oxygen species. *J. Neurosci.* **24:**7779-7788; 2004.

[8] Tretter, L.; Adam-Vizi, V. Generation of reactive oxygen species in the reaction catalyzed by alpha-ketoglutarate dehydrogenase. *J. Neurosci.* **24:**7771-7778; 2004.

[9] Babady, N. E.; Pang, Y. P.; Elpeleg, O.; Isaya, G. Cryptic proteolytic activity of dihydrolipoamide dehydrogenase. *Proc. Natl. Acad. Sci. USA* **104:**6158-6163; 2007.

[10] Tyagi, T. K.; Ponnan, P.; Singh, P.; Bansal, S.; Batra, A.; Collin, F.; Guillonneau, F.; Jore, D.; Patkar, S. A.; Saxena, R. K.; Parmar, V. S.; Rastogi, R. C.; Raj, H. G. Moonlighting protein in Starkeyomyces koorchalomoides: Characterization of dihydrolipoamide dehydrogenase as a protein acetyltransferase utilizing acetoxycoumarin as the acetyl group donor. *Biochimie* **91:**868-875; 2009.

[11] Fisher-Wellman, K. H.; Gilliam, L. A. A.; Lin, C. T.; Cathey, B. L.; Lark, D. S.; Neufer, P. D. Mitochondrial glutathione depletion reveals a novel role for the pyruvate dehydrogenase complex as a key H2O2-emitting source under conditions of nutrient overload. *Free Radic. Biol. Med.* **65:**1201-1208; 2013.

[12] Nemeria, N. S.; Ambrus, A.; Patel, H.; Gerfen, G.; Adam-Vizi, V.; Tretter, L.; Zhou, J.; Wang, J.; Jordan, F. Human 2-Oxoglutarate Dehydrogenase Complex E1 Component Forms a Thiamin-derived Radical by Aerobic Oxidation of the Enamine Intermediate. *J. Biol. Chem.* **289:**29859-29873; 2014.

[13] Quinlan, C. L.; Goncalves, R. L.; Hey-Mogensen, M.; Yadava, N.; Bunik, V. I.; Brand, M. D. The 2-oxoacid dehydrogenase complexes in mitochondria can produce superoxide/hydrogen peroxide at much higher rates than complex I. *J Biol Chem* **289:**8312-8325; 2014.

[14] Starkov, A. A. An update on the role of mitochondrial alpha-ketoglutarate dehydrogenase in oxidative stress. *Molecular and Cellular Neuroscience* **55:**13-16; 2013.

[15] Adam-Vizi, V.; Tretter, L. The role of mitochondrial dehydrogenases in the generation of oxidative stress. *Neurochem. Int.* **62:**757-763; 2013.

[16] Berg, A.; deKok, A. 2-oxo acid dehydrogenase multienzyme complexes. The central role of the lipoyl domain. *Biol. Chem.* **378:**617-634; 1997.

[17] Guest, J. R.; Darlison, M. G.; Spencer, M. E.; Stephens, P. E. Cloning and sequence analysis of the pyruvate and 2-oxoglutarate dehydrogenase complex genes of Escherichia coli. *Biochem. Soc. Trans.* **12:**220-223; 1984.

[18] Koike, K. Cloning, structure, chromosomal localization and promoter analysis of human 2-oxoglutarate dehydrogenase gene. *Biochimica Et Biophysica Acta-Protein Structure and Molecular Enzymology* **1385:**373-384; 1998.
[19] Koike, K.; Ohta, S.; Urata, Y.; Kagawa, Y.; Koike, M. Cloning and sequencing of cDNAs encoding alpha-subunits and beta-subunits of human pyruvate dehydrogenase. *Proc. Natl. Acad. Sci. USA* **85:**41-45; 1988.
[20] Thekkumkara, T. J.; Jesse, B. W.; Ho, L.; Raefsky, C.; Pepin, R. A.; Javed, A. A.; Pons, G.; Patel, M. S. Isolation of a cDNA clone for the dihydrolipoamide acetyltransferase component of the human liver pyruvate dehydrogenase complex. *Biochem. Biophys. Res. Commun.* **145:**903-907; 1987.
[21] Nakano, K.; Takase, C.; Sakamoto, T.; Nakagawa, S.; Inazawa, J.; Ohta, S.; Matuda, S. Isolation, characterization and structural organization of the gene and pseudogene for the dihydrolipoamide succinyltransferase component of the human 2-oxoglutarate dehydrogenase complex. *Eur. J. Biochem.* **224:**179-189; 1994.
[22] Otulakowski, G.; Robinson, B. H.; Willard, H. F. Gene for lipoamide dehydrogenase maps to human chromosome 7. *Somatic Cell and Molecular Genetics* **14:**411-414; 1988.
[23] Brown, J. P.; Perham, R. N. An amino acid sequence in the active site of lipoamide dehydrogenase from the 2-oxoglutarate dehydrogenase complex of *E. coli* (Crookes strain). *FEBS Letters* **26:**221-224; 1972.
[24] Pettit, F. H.; Reed, L. J. Alpha-keto acid dehydrogenase complexes. 8. Comparison of dihydrolipoyl dehydrogenases from pyruvate and alpha-ketoglutarate dehydrogenase complexes of *Escherichia coli*. *Proc. Natl. Acad. Sci. USA* **58:**1126-1130; 1967.
[25] Reed, L. J.; Hackert, M. L. Structure-function relationships in dihydrolipoamide acyltransferases. *J. Biol. Chem.* **265:**8971-8974; 1990.
[26] Huennekens, F. M.; Basford, R. E.; Gabrio, B. W. An oxidase for reduced diphosphopyridine nucleotide. *J. Biol. Chem.* **213:**951-967; 1955.
[27] Ambrus, A.; Tretter, L.; Adam-Vizi, V. Inhibition of the alpha-ketoglutarate dehydrogenase-mediated reactive oxygen species generation by lipoic acid. *J. Neurochem.* **109:**222-229; 2009.
[28] Tretter, L.; Adam-Vizi, V. Alpha-ketoglutarate dehydrogenase: a target and generator of oxidative stress. *Philos. Trans. R. Soc. B-Biol. Sci.* **360:**2335-2345; 2005.
[29] Adam-Vizi, V. Production of reactive oxygen species in brain mitochondria: Contribution by electron transport chain and non-electron transport chain sources. *Antioxid. Redox Signal.* **7:**1140-1149; 2005.
[30] Adam-Vizi, V.; Chinopoulos, C. Bioenergetics and the formation of mitochondrial reactive oxygen species. *Trends in Pharmacological Sciences* **27:**639-645; 2006.
[31] Tahara, E. B.; Barros, M. H.; Oliveira, G. A.; Netto, L. E. S.; Kowaltowski, A. J. Dihydrolipoyl dehydrogenase as a source of reactive oxygen species inhibited by caloric restriction and involved in Saccharomyces cerevisiae aging. *Faseb J.* **21:**274-283; 2007.
[32] Bunik, V. I.; Schloss, J. V.; Pinto, J. T.; Gibson, G. E.; Cooper, A. J. L. Enzyme-catalyzed side reactions with molecular oxygen may contribute to cell signaling and neurodegenerative diseases. *Neurochem. Res.* **32:**871-891; 2007.
[33] Zundorf, G.; Kahlert, S.; Bunik, V. I.; Reiser, G. Alpha-ketoglutarate dehydrogenase contributes to production of reactive oxygen species in glutamate-stimulated hippocampal neurons in situ *Neuroscience* **158:**610-616; 2009.
[34] Graf, A.; Kabysheva, M.; Klimuk, E.; Trofimova, L.; Dunaeva, T.; Zundorf, G.; Kahlert, S.; Reiser, G.; Storozhevykh, T.; Pinelis, V.; Sokolova, N.; Bunik, V. Role of 2-oxoglutarate

dehydrogenase in brain pathologies involving glutamate neurotoxicity. *J. Mol. Catal. B-Enzym.* **61:**80-87; 2009.
[35] Starkov, A. A.; Adam-Vizi, V. Calcium and mitochondrial reactive oxygen species generation: how to read the facts. *J. Alzheim. Dis.* **20:**S413-426; 2010.
[36] Gibson, G. E.; Starkov, A.; Blass, J. P.; Ratan, R. R.; Beal, M. F. Cause and consequence: Mitochondrial dysfunction initiates and propagates neuronal dysfunction, neuronal death and behavioral abnormalities in age-associated neurodegenerative diseases. *Biochim. Biophys. Acta-Mol. Basis Dis.* **1802:**122-134; 2010.
[37] Ambrus, A.; Torocsik, B.; Tretter, L.; Ozohanics, O.; Adam-Vizi, V. Stimulation of reactive oxygen species generation by disease-causing mutations of lipoamide dehydrogenase. *Hum. Mol. Genet.* **20:**2984–2995; 2011.
[38] Chinopoulos, C.; Tretter, L.; Adam-Vizi, V. Depolarization of In Situ Mitochondria Due to Hydrogen Peroxide-Induced Oxidative Stress in Nerve Terminals. *J. Neurochem.* **73:**220-228; 1999.
[39] Tretter, L.; Adam-Vizi, V. Inhibition of Krebs cycle enzymes by hydrogen peroxide: A key role of alpha-ketoglutarate dehydrogenase in limiting NADH production under oxidative stress. *J. Neurosci.* **20:**8972-8979; 2000.
[40] Nulton-Persson, A. C.; Szweda, L. I. Modulation of mitochondrial function by hydrogen peroxide. *J. Biol. Chem.* **276:**23357-23361; 2001.
[41] Kumar, M. J.; Nicholls, D. G.; Andersen, J. K. Oxidative alpha-ketoglutarate dehydrogenase inhibition via subtle elevations in monoamine oxidase B levels results in loss of spare respiratory capacity - Implications for Parkinson's disease. *J. Biol. Chem.* **278:**46432-46439; 2003.
[42] Ambrus, A.; Adam-Vizi, V. Molecular dynamics study of the structural basis of dysfunction and the modulation of reactive oxygen species generation by pathogenic mutants of human dihydrolipoamide dehydrogenase. *Arch. Biochem. Biophys.* **538:**145-155; 2013.
[43] Vereczki, V.; Martin, E.; Rosenthal, R. E.; Hof, P. R.; Hoffman, G. E.; Fiskum, G. Normoxic resuscitation after cardiac arrest protects against hippocampal oxidative stress, metabolic dysfunction, and neuronal death. *J. Cereb. Blood Flow Metab.* **26:**821-835; 2006.
[44] Contreras, N. D.; Vasquez, C. C. Tellurite-induced carbonylation of the Escherichia coli pyruvate dehydrogenase multienzyme complex. *Archives of Microbiology* **192:**969-973; 2010.
[45] Vaubel, R. A.; Rustin, P.; Isaya, G. Mutations in the Dimer Interface of Dihydrolipoamide Dehydrogenase Promote Site-specific Oxidative Damages in Yeast and Human Cells. *J. Biol. Chem.* **286:**40232-40245; 2011.
[46] Klyachko, N. L.; Shchedrina, V. A.; Efimov, A. V.; Kazakov, S. V.; Gazaryan, I. G.; Kristal, B. S.; Brown, A. M. pH-dependent substrate preference of pig heart lipoamide dehydrogenase varies with oligomeric state - Response to mitochondrial matrix acidification. *J. Biol. Chem.* **280:**16106-16114; 2005.
[47] Gazaryan, I. G.; Krasnikov, B. F.; Ashby, G. A.; Thorneley, R. N. F.; Kristal, B. S.; Brown, A. M. Zinc is a potent inhibitor of thiol oxidoreductase activity and stimulates reactive oxygen species production by lipoamide dehydrogenase. *J. Biol. Chem.* **277:**10064-10072; 2002.
[48] Bando, Y.; Aki, K. Mechanisms of generation of oxygen radicals and reductive mobilization of ferritin iron by lipoamide dehydrogenase. *J. Biochem.* **109:**450-454; 1991.
[49] Massey, V.; Strickland, S.; Mayhew, S. G.; Howell, L. G.; Engel, P. C.; Matthews, R. G.; Schuman, M.; Sullivan, P. A. The production of superoxide anion radicals in the reaction of reduced flavins and flavoproteins with molecular oxygen. *Biochem. Biophys. Res. Commun.* **36:**891-897; 1969.

[50] Ambrus, A.; Mizsei, R.; Adam-Vizi, V. Structural alterations by five disease-causing mutations in the low-pH conformation of human dihydrolipoamide dehydrogenase (hLADH) analyzed by molecular dynamics – Implications in functional loss and modulation of reactive oxygen species generation by pathogenic hLADH forms. *Biochem. Biophys. Reports* **2:**50-56; 2015.
[51] Quinonez, S. C.; Leber, S. M.; Martin, D. M.; Thoene, J. G.; Bedoyan, J. K. Leigh Syndrome in a Girl With a Novel DLD Mutation Causing E3 Deficiency. *Pediatr. Neurol.* **48:**67-72; 2013.
[52] Frank, R. A. W.; Kay, C. W. M.; Hirsi, J.; Luisi, B. F. Off-pathway, oxygen-dependent thiamine radical in the Krebs cycle. *J. Am. Chem. Soc.* **130:**1662-1668; 2008.
[53] Reed, G. H.; Ragsdale, S. W.; Mansoorabadi, S. O. Radical reactions of thiamin pyrophosphate in 2-oxoacid oxidoreductases. *Biochimica Et Biophysica Acta-Proteins and Proteomics* **1824:**1291-1298; 2012.
[54] Reed, L. J.; Oliver, R. M. The multienzyme alpha-keto acid dehydrogenase complexes. *Brookhaven Symp. Biol.* **21:**397-412; 1968.
[55] Erfle, J. D.; Sauer, F. The inhibitory effects of acyl-coenzyme A esters on the pyruvate and a-oxoglutarate dehydrogenase complexes. *Biochim. Biophys. Acta* **178:**441-452; 1969.
[56] Poulsen, L. L.; Wedding, R. T. Purification and properties of the a-ketoglutarate dehydrogenase complex of cauliflower mitochondria. *J. Biol. Chem.* **245:**5709-5717; 1970.
[57] Constantinescu, A.; Pick, U.; Handelman, G. J.; Haramaki, N.; Han, D.; Podda, M.; Tritschler, H. J.; Packer, L. Reduction and transport of lipoic acid by human erythrocytes. *Biochem. Pharmacol.* **50:**253-261; 1995.
[58] Yan, L. J.; Thangthaeng, N.; Sumien, N.; Forster, M. J. Serum Dihydrolipoamide Dehydrogenase Is a Labile Enzyme. *J Biochem Pharmacol Res* **1:**30-42; 2013.
[59] Mottley, C.; Mason, R. P. Sulfur-centered radical formation from the antioxidant dihydrolipoic acid. *J. Biol. Chem.* **276:**42677-42683; 2001.
[60] Nemeria, N.; Volkov, A.; Brown, A.; Yi, J.; Zipper, L.; Guest, J. R.; Jordan, F. Systematic study of the six cysteines of the E1 subunit of the pyruvate dehydrogenase multienzyme complex from Escherichia coli: None is essential for activity. *Biochemistry* **37:**911-922; 1998.
[61] Song, J.; Park, Y. H.; Nemeria, N.; Kale, S.; Kakalis, L.; Jordan, F. Nuclear magnetic resonance evidence for the role of the flexible regions of the E1 component of the pyruvate dehydrogenase complex from gram-negative bacteria. *J. Biol. Chem.* **285:**4680-4694; 2010.
[62] Wei, W.; Li, H.; Nemeria, N.; Jordan, F. Expression and purification of the dihydrolipoamide acetyltransferase and dihydrolipoamide dehydrogenase subunits of the Escherichia coli pyruvate dehydrogenase multienzyme complex: a mass spectrometric assay for reductive acetylation of dihydrolipoamide acetyltransferase. *Protein Expr. Purif.* **28:**140-150; 2003.
[63] Shim, D. J.; Nemeria, N. S.; Balakrishnan, A.; Patel, H.; Song, J.; Wang, J. J.; Jordan, F.; Farinas, E. T. Assignment of Function to Histidines 260 and 298 by Engineering the E1 Component of the Escherichia coli 2-Oxoglutarate Dehydrogenase Complex; Substitutions That Lead to Acceptance of Substrates Lacking the 5-Carboxyl Group. *Biochemistry* **50:**7705-7709; 2011.
[64] Korotchkina, L. G.; Tucker, M. M.; Thekkumkara, T. J.; Madhusudhan, K. T.; Pons, G.; Kim, H. J.; Patel, M. S. Overexpression and characterization of human tetrameric pyruvate dehydrogenase and its individual subunits. *Protein Expr. Purif.* **6:**79-90; 1995.
[65] Korotchkina, L. G.; Patel, M. S. Probing the mechanism of inactivation of human pyruvate dehydrogenase by phosphorylation of three sites. *J. Biol. Chem.* **276:**5731-5738; 2001.

[66] Yang, D. Q.; Song, J. S.; Wagenknecht, T.; Roche, T. E. Assembly and full functionality of recombinantly expressed dihydrolipoyl acetyltransferase component of the human pyruvate dehydrogenase complex. *J. Biol. Chem.* **272:**6361-6369; 1997.
[67] Harris, R. A.; BowkerKinley, M. M.; Wu, P. F.; Jeng, J. J.; Popov, K. M. Dihydrolipoamide dehydrogenase-binding protein of the human pyruvate dehydrogenase complex - DNA-derived amino acid sequence, expression, and reconstitution of the pyruvate dehydrogenase complex. *J. Biol. Chem.* **272:**19746-19751; 1997.
[68] Ambrus, A.; Torocsik, B.; Adam-Vizi, V. Periplasmic cold expression and one-step purification of human dihydrolipoamide dehydrogenase. *Protein Expr. Purif.* **63:**50-57; 2009.
[69] Balakrishnan, A.; Nemeria, N. S.; Chakraborty, S.; Kakalis, L.; Jordan, F. Determination of pre-steady-state constants on the Escherichia coli pyruvate dehydrogenase complex reveals that loop movement controls the rate-limiting step. *J. Am. Chem. Soc.* **134:**18644-18655; 2012.
[70] Yi, J. Z.; Nemeria, N.; McNally, A.; Jordan, F.; Machado, R. S.; Guest, J. R. Effect of substitutions in the thiamin diphosphate-magnesium fold on the activation of the pyruvate dehydrogenase complex from Escherichia coli by cofactors and substrate. *J. Biol. Chem.* **271:**33192-33200; 1996.
[71] Saumweber, H.; Binder, R.; Bisswanger, H. Pyruvate dehydrogenase component of the pyruvate dehydrogenase complex from Escherichia coli K-12 - purification and characterization. *Eur. J. Biochem.* **114:**407-411; 1981.
[72] Nemeria, N.; Yan, Y.; Zhang, Z.; Brown, A. M.; Arjunan, P.; Furey, W.; Guest, J. R.; Jordan, F. Inhibition of the Escherichia coli pyruvate dehydrogenase complex E1 subunit and its tyrosine 177 variants by thiamin 2-thiazolone and thiamin 2-thiothiazolone diphosphates - Evidence for reversible tight-binding inhibition. *J. Biol. Chem.* **276:**45969-45978; 2001.
[73] Gupta, S. C.; Dekker, E. E. Evidence for the identity and some comparative properties of alpha-ketoglutarate and 2-keto-4-hydroxyglutarate dehydrogenase activity. *J. Biol. Chem.* **255:**1107-1112; 1980.
[74] Hirashima, M.; Hayakawa, T.; Koike, M. Mammalian alpha-keto acid dehydrogenase complexes. II. An improved procedure for the preparation of 2-oxoglutarate dehydrogenase complex from pig heart muscle. *J. Biol. Chem.* **242:**902-907; 1967.
[75] Hamada, M.; Koike, K.; Nakaula, Y.; Hiraoka, T.; Koike, M. A kinetic study of the alpha-keto acid dehydrogenase complexes from pig heart mitochondria. *J. Biochem.* **77:**1047-1056; 1975.
[76] Hansford, R. G. Control of mitochondrial substrate oxidation. *Curr. Top. Bioenerg.* **10:**217-278; 1980.
[77] Kiselevsky, Y. V.; Ostrovtsova, S. A.; Strumilo, S. A. Kinetic characterization of the pyruvate and oxoglutarate dehydrogenase complexes from human heart. *Acta Biochim Pol* **37:**135-139; 1990.
[78] Seifert, F.; Golbik, R.; Brauer, J.; Lilie, H.; Schroder-Tittmann, K.; Hinze, E.; Korotchkina, L. G.; Patel, M. S.; Tittmann, K. Direct kinetic evidence for half-of-the-sites reactivity in the E1 component of the human pyruvate dehydrogenase multienzyme complex through alternating sites cofactor activation. *Biochemistry* **45:**12775-12785; 2006.
[79] Popov, V. O.; Gazaryan, I. G.; Egorov, A. M.; Berezin, I. V. NAD-dependent hydrogenase from the hydrogen-oxidizing bacterium Alcaligenes Eutrophus Z1 - kinetic studies of the NADH-dehydrogenase activity. *Biochim. Biophys. Acta* **827:**466-471; 1985.
[80] Mayo, L. A.; Curnutte, J. T. KInetic microplate assay for superoxide production by neutrophils and other phagocytic cells. *Method Enzymol.* **186:**567-575; 1990.

[81] Azzi, A.; Montecucco, C.; Richter, C. Use of acetylated ferricytochrome c for detection of superoxide radicals produced in biological membranes. *Biochem. Biophys. Res. Commun.* **65:**597-603; 1975.
[82] McCord, J. M.; Fridovich, I. The reduction of cytochrome c by milk xantine oxidase. *J. Biol. Chem.* **243:**5753-5760; 1968.
[83] Rosen, G. M.; Finkelstein, E.; Rauckman, E. J. A method for the detection of superoxide in biological systems. *Arch. Biochem. Biophys.* **215:**367-378; 1982.
[84] Cameron, J. M.; Levandovskiy, V.; MacKay, N.; Raiman, J.; Renaud, D. L.; Clarke, J. T. R.; Feigenbaum, A.; Elpeleg, O.; Robinson, B. H. Novel mutations in dihydrolipoamide dehydrogenase deficiency in two cousins with borderline-normal PDH complex activity. *Am. J. Med. Genet. A* **140A:**1542-1552; 2006.
[85] Brautigam, C. A.; Chuang, J. L.; Tomchick, D. R.; Machius, M.; Chuang, D. T. Crystal structure of human dihydrolipoamide dehydrogenase: NAD(+)/NADH binding and the structural basis of disease-causing mutations. *J. Mol. Biol.* **350:**543-552; 2005.
[86] Massey, V. Activation of molecular oxygen by flavins and flavoproteins. *J. Biol. Chem.* **269:**22459-22462; 1994.
[87] Tretter, L.; Ambrus, A. Measurement of ROS homeostasis in isolated mitochondria. *Methods Enzymol* **547:**199-223; 2014.
[88] Bunik, V. I.; Sievers, C. Inactivation of the 2-oxo acid dehydrogenase complexes upon generation of intrinsic radical species. *Eur. J. Biochem.* **269:**5004-5015; 2002.
[89] Starkov, A. A. The Role of Mitochondria in Reactive Oxygen Species Metabolism and Signaling. In: Gibson, G. E.; Ratan, R. R.; Beal, M. F., eds. *Mitochondria and Oxidative Stress in Neurodegenerative Disorders*; 2008: 37-52.
[90] Droge, W.; Schipper, H. M. Oxidative stress and aberrant signaling in aging and cognitive decline. *Aging Cell* **6:**361-370; 2007.
[91] Tretter, L.; Sipos, I.; Adam-Vizi, V. Initiation of neuronal damage by complex I deficiency and oxidative stress in Parkinson's disease. *Neurochem. Res.* **29:**569-577; 2004.
[92] Gibson, G. E.; Kingsbury, A. E.; Xu, H.; Lindsay, J. G.; Daniel, S.; Foster, O. J. F.; Lees, A. J.; Blass, J. P. Deficits in a tricarboxylic acid cycle enzyme in brains from patients with Parkinson's disease. *Neurochem. Int.* **43:**129-135; 2003.
[93] Brookes, P. S., ed. *Mitochondrial production of oxidants and their role in the regulation of cellular processes.* 2007.
[94] Martinvalet, D.; Zhu, P. C.; Lieberman, J. Granzyme A induces caspase-independent mitochondrial damage, a required first step for apoptosis. *Immunity* **22:**355-370; 2005.
[95] Chinopoulos, C.; Adam-Vizi, V. Calcium, mitochondria and oxidative stress in neuronal pathology - Novel aspects of an enduring theme. *Febs J.* **273:**433-450; 2006.
[96] Lai, J. C. K.; Walsh, J. M.; Dennis, S. C.; Clark, J. B. Synaptic and non-synaptic mitochondria from rat brain isolation and characterization. *J. Neurochem.* **28:**625-631; 1977.
[97] Blass, J. P. Metabolic alterations common to neural and non-neural cells in Alzheimer's disease. *Hippocampus* **13:**45-54; 1993.
[98] Willems, H. L.; de Kort, T. F.; Trijbels, F. J.; Monnens, L. A.; Veerkamp, J. H. Determination of pyruvate oxidation rate and citric acid cycle activity in intact human leukocytes and fibroblasts. *Clinical Chemistry* **24:**200-203; 1978.
[99] Kussmaul, L.; Hirst, J. The mechanism of superoxide production by NADH:ubiquinone oxidoreductase (complex I) from bovine heart mitochondria. *Proc Natl Acad Sci U S A* **103:**7607-7612; 2006.

[100] McLennan, H. R.; Degli Esposti, M. The contribution of mitochondrial respiratory complexes to the production of reactive oxygen species. *J Bioenerg Biomembr* **32:**153-162; 2000.
[101] Siebels, I.; Drose, S. Q-site inhibitor induced ROS production of mitochondrial complex II is attenuated by TCA cycle dicarboxylates. *Biochim Biophys Acta* **1827:**1156-1164; 2013.
[102] Lakaschus, G.; Loffler, M. Differential susceptibility of dihydroorotate dehydrogenase/oxidase to Brequinar Sodium (NSC 368 390) in vitro. *Biochem Pharmacol* **43:**1025-1030; 1992.
[103] Andreyev, A. Y.; Kushnareva, Y. E.; Murphy, A. N.; Starkov, A. A. Mitochondrial ROS metabolism: 10 Years later. *Biochemistry-Moscow* **80:**517-531; 2015.
[104] Tretter, L.; Adam-Vizi, V. Moderate dependence of ROS formation on Delta psi m in isolated brain mitochondria supported by NADH-linked substrates. *Neurochem. Res.* **32:**569-575; 2007.
[105] Tretter, L.; Adam-Vizi, V. Uncoupling is without an effect on the production of reactive oxygen species by in situ synaptic mitochondria. *J. Neurochem.* **103:**1864-1871; 2007.
[106] Tretter, L.; Adam-Vizi, V. High Ca2+ load promotes Hydrogen peroxide generation via activation of alpha-glycerophosphate dehydrogenase in brain mitochondria. *Free Radic. Biol. Med.* **53:**2119-2130; 2012.
[107] Tretter, L.; Liktor, B.; Adam-Vizi, V. Dual effect of pyruvate in isolated nerve terminals: Generation of reactive oxygen species and protection of aconitase. *Neurochem. Res.* **30:**1331-1338; 2005.
[108] Tretter, L.; Mayer-Takacs, D.; Adam-Vizi, V. The effect of bovine serum albumin on the membrane potential and reactive oxygen species generation in succinate-supported isolated brain mitochondria. *Neurochem. Int.* **50:**139-147; 2007.
[109] Tretter, L.; Takacs, K.; Hegedus, V.; Adam-Vizi, V. Characteristics of alpha-glycerophosphate-evoked H2O2 generation in brain mitochondria. *J. Neurochem.* **100:**650-663; 2007.
[110] Tretter, L.; Takacs, K.; Kover, K.; Adam-Vizi, V. Stimulation of H2O2 generation by calcium in brain mitochondria respiring on alpha-glycerophosphate. *J. Neurosci. Res.* **85:**3471-3479; 2007.
[111] Shi, Q. L.; Chen, H. L.; Xu, H.; Gibson, G. E. Reduction in the E2k subunit of the alpha-ketoglutarate dehydrogenase complex has effects independent of complex activity. *J. Biol. Chem.* **280:**10888-10896; 2005.
[112] Gibson, G. E.; Zhang, H.; Sheu, K. F. R.; Bogdanovich, N.; Lindsay, J. G.; Lannfelt, L.; Vestling, M.; Cowburn, R. F. alpha-ketoglutarate dehydrogenase in Alzheimer brains bearing the APP670/671 mutation. *Ann. Neurol.* **44:**676-681; 1998.
[113] Cruts, M.; Backhovens, H.; Vangassen, G.; Theuns, J.; Wang, S. Y.; Wehnert, A.; Vanduijn, C. M.; Karlsson, T.; Hofman, A.; Adolfsson, R.; Martin, J. J.; Vanbroeckhoven, C. Mutation analysis of the chromosome 14q24.3 dihydrolipoyl succinyltransferase (dlst) gene in patients with early-onset Alzheimer-disease. *Neuroscience Letters* **199:**73-77; 1995.
[114] Dumont, M.; Ho, D. J.; Calingasan, N. Y.; Xu, H.; Gibson, G.; Beal, M. F. Mitochondrial dihydrolipoyl succinyltransferase deficiency accelerates amyloid pathology and memory deficit in a transgenic mouse model of amyloid deposition. *Free Radic. Biol. Med.* **47:**1019-1027; 2009.
[115] Diaz-Munoz, M. D.; Bell, S. E.; Fairfax, K.; Monzon-Casanova, E.; Cunningham, A. F.; Gonzalez-Porta, M.; Andrews, S. R.; Bunik, V. I.; Zarnack, K.; Curk, T.; Heggermont, W. A.; Heymans, S.; Gibson, G. E.; Kontoyiannis, D. L.; Ule, J.; Turner, M. The RNA-binding protein HuR is essential for the B cell antibody response. *Nature Immunology* **16:**415-425; 2015.

[116] Shaag, A.; Saada, A.; Berger, I.; Mandel, H.; Joseph, A.; Feigenbaum, A.; Elpeleg, O. N. Molecular basis of lipoamide dehydrogenase deficiency in Ashkenazi Jews. *Am. J. Med. Genet.* **82:**177-182; 1999.
[117] Hong, Y. S.; Korman, S. H.; Lee, J.; Ghoshal, P.; Qu, Q.; Barash, V.; Kang, S.; Oh, S.; Kwon, M.; Gutman, A.; Rachmel, A.; Patel, M. S. Identification of a common mutation (Gly194Cys) in both Arab Moslem and Ashkenazi Jewish patients with dihydrolipoamide dehydrogenase (E3) deficiency: Possible beneficial effect of vitamin therapy. *J. Inherit. Metab. Dis.* **26:**816-818; 2003.
[118] Shany, E.; Saada, A.; Landau, D.; Shaag, A.; Hershkovitz, E.; Elpeleg, O. N. Lipoamide dehydrogenase deficiency due to a novel mutation in the interface domain. *Biochem. Biophys. Res. Commun.* **262:**163-166; 1999.
[119] Brautigam, C. A.; Wynn, R. M.; Chuang, J. L.; Machius, M.; Tomchick, D. R.; Chuang, D. T. Structural insight into interactions between dihydrolipoamide dehydrogenase (E3) and E3 binding protein of human pyruvate dehydrogenase complex. *Structure* **14:**611-621; 2006.

**Table 1**. Activities of the *E. coli* and human PDHc and OGDHc and their components at optimal stoichiometry.

| Enzyme | Overall complex activity ($\mu mol \cdot min^{-1} \cdot mg\ E3^{-1}$) | Superoxide activity (forward) ($\mu mol \cdot min^{-1} \cdot mg\ E3^{-1}$) | Superoxide activity (reverse) ($\mu mol \cdot min^{-1} \cdot mg\ E3^{-1}$) |
|---|---|---|---|
| hPDHc | 37.0 ± 1.1 | 0.057 ± 0.001 | 0.108 ± 0.001 |
| hE3 | _ | _ | 0.096 ± 0.003 |
| hOGDHc | 0.625 ± 0.005 | 0.012 ± 0.000 | 0.040 ± 0.001 |
| hE1o | _ | 0.0021 ± 0.0001 ($\mu mol \cdot min^{-1} \cdot mg\ E1o^{-1}$) | _ |
| ecPDHc | 34.7 ± 2.2 | 0.041 ± 0.004 | 0.062 ± 0.003 |
| ecE3 | _ | _ | 0.075 ± 0.007 |
| ecOGDHc | 3.71 ± 0.10 | 0.019 ± 0.001 | 0.045 ± 0.000 |

Figure 1

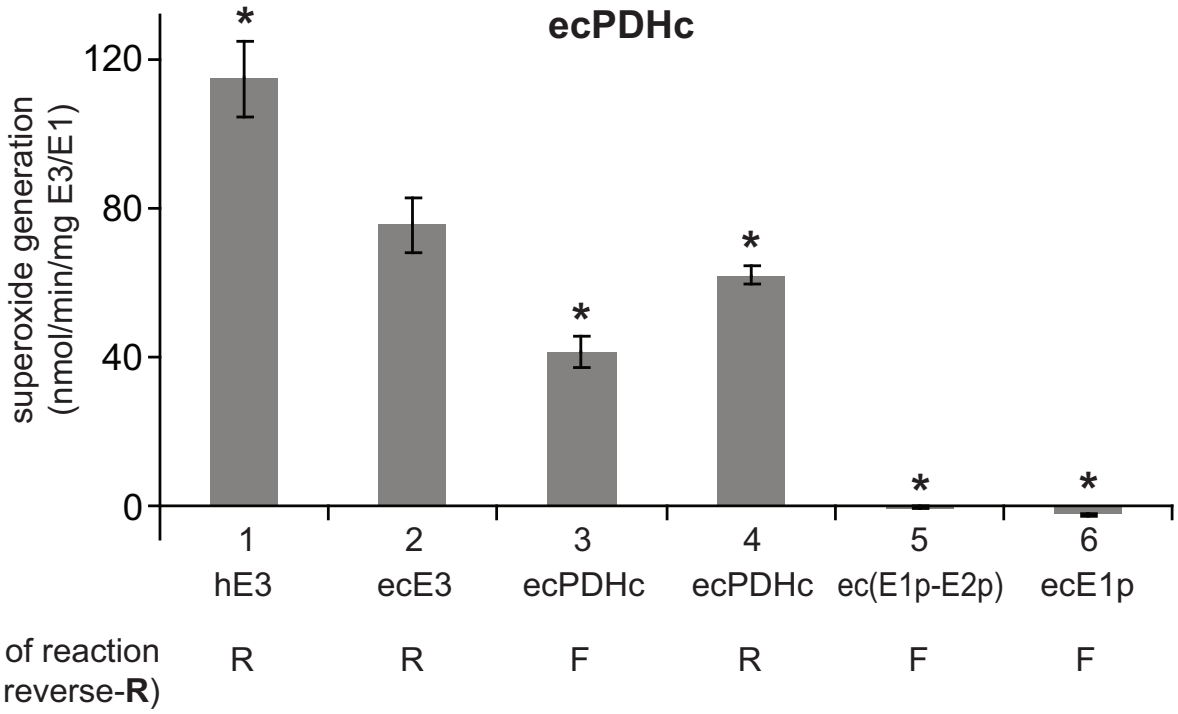


**Figure 1.**

Figure 2

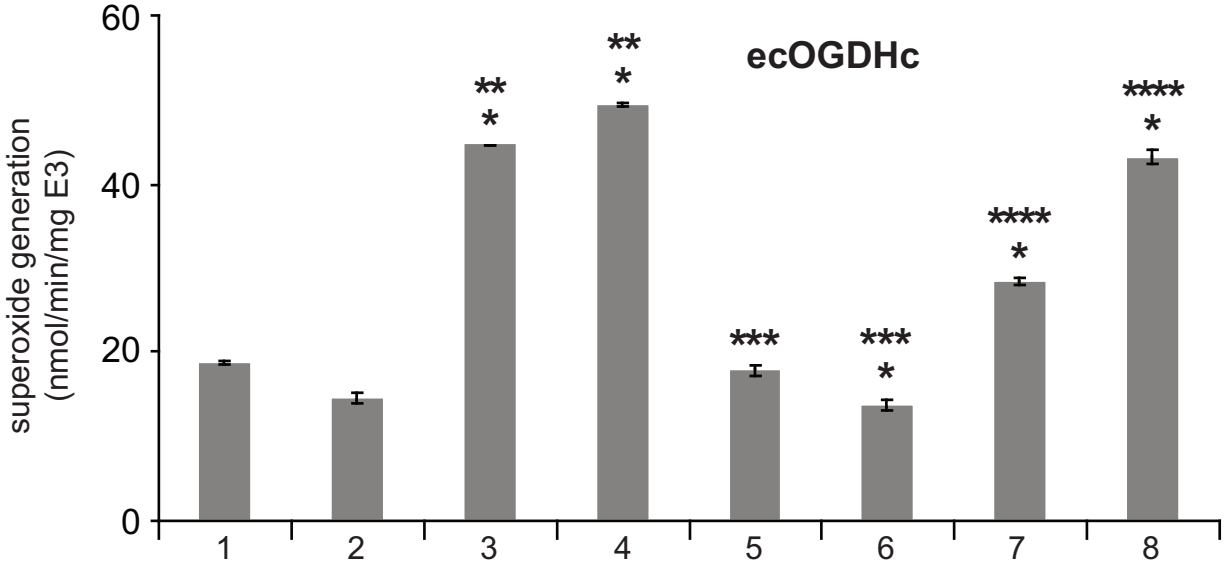


**Figure 2.**

**Figure 3**

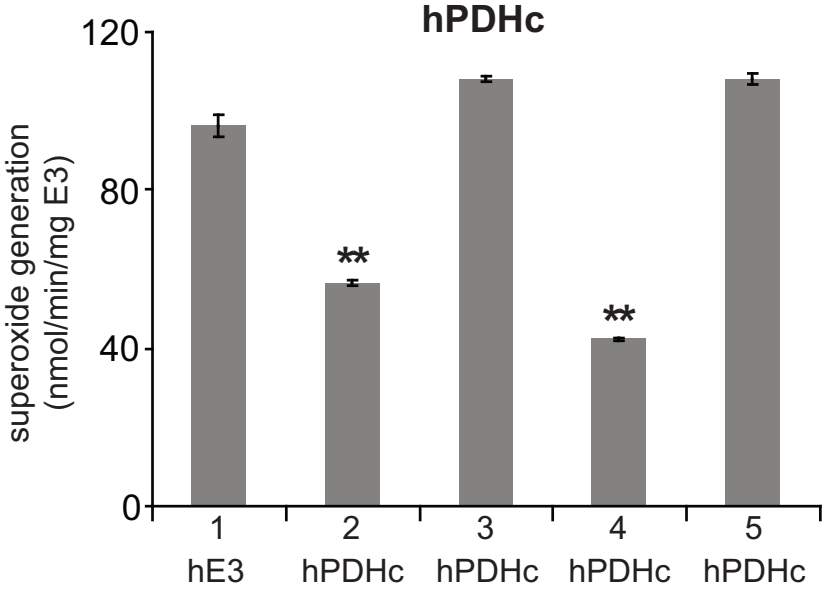


| | | | | | |
|---|---|---|---|---|---|
| direction of reaction (forward-**F**, reverse-**R**) | R | F# | R | F | R |
| E3 component (**a**: WT; **b**: G194C) | a | a | a | b | b |

Figure 3.

**Figure 4**

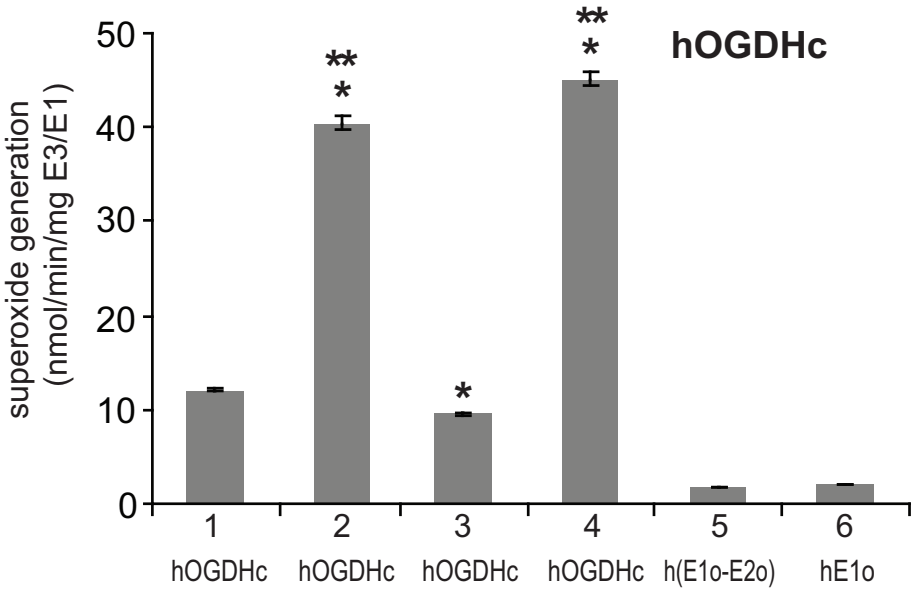


| | | | | | | |
|---|---|---|---|---|---|---|
| direction of reaction (forward-**F**, reverse-**R**) | F | R | F | R | F# | F# |
| E3 component (**a**: WT; **b**: G194C) | a | a | b | b | - | - |

Figure 4.

**Scheme 1**

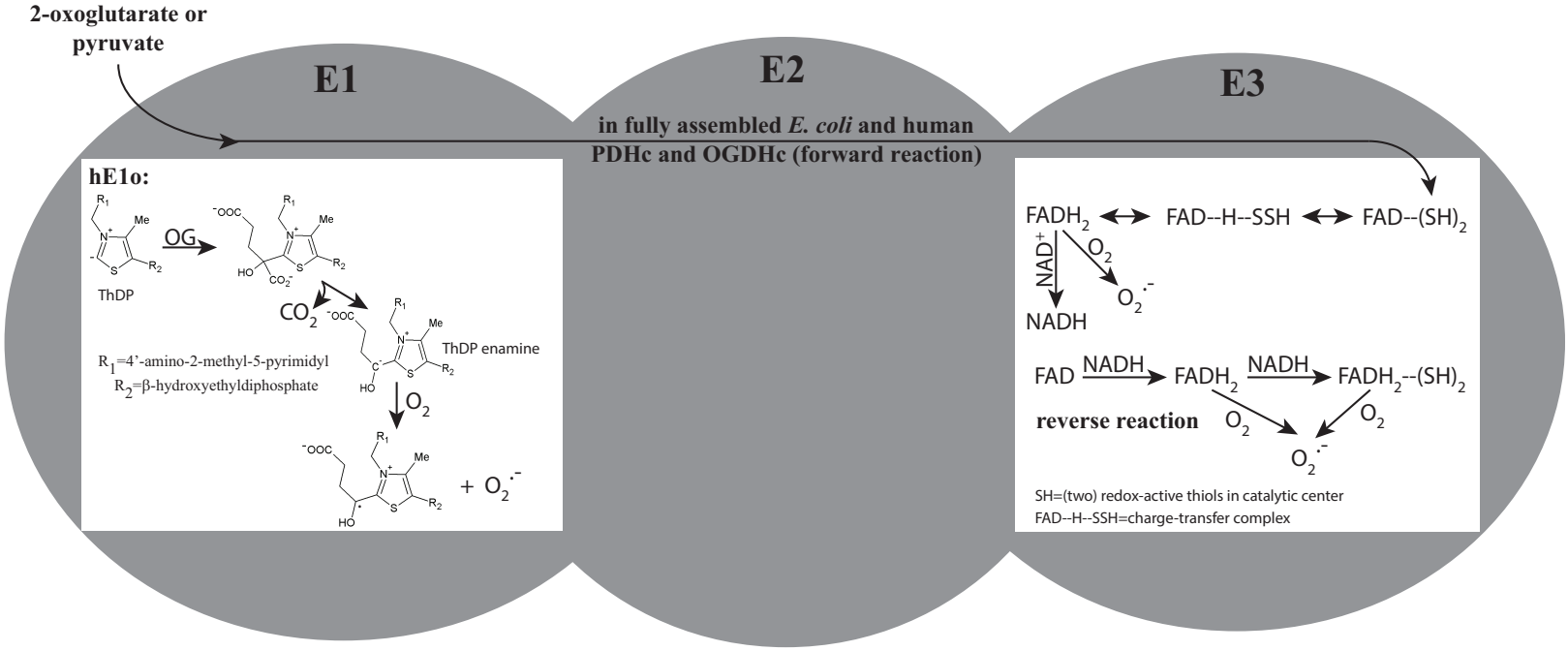


Scheme 1.